

Toward understanding the S₂-S₃ transition in the Kok Cycle of Photosystem II: Lessons from Sr-Substituted Structure

Muhammed Amin^{1,2,3*}, Divya Kaur^{4,5,6}, M.R. Gunner^{5,6}, Gary Brudvig⁷

¹ Rijksuniversiteit Groningen Biomolecular Sciences and Biotechnology Institute, University of Groningen, Groningen, Netherlands

² Physics Department, University College Groningen, University of Groningen, Groningen, Netherlands

³ Centre for Theoretical Physics, The British University in Egypt, Sherouk City 11837, Cairo, Egypt

⁴ Department of Physics and Department of Chemistry, Brock University, 500 Glenridge Avenue, St. Catharines, ON Canada L2S 3A1

⁵ Department of Chemistry, The Graduate Center of the City University of New York, New York, NY 10016, United States

⁶ Department of Physics, City College of New York, New York, NY 10031, United States

⁷ Department of Chemistry, Yale University, New Haven, Connecticut 06520-8107, United States

m.a.a.amin@rug.nl

ABSTRACT: Understanding the water oxidation mechanism in Photosystem II (PSII) stimulates the design of biomimetic artificial systems that can convert solar energy into hydrogen fuel efficiently. The Sr²⁺ substituted PSII is active but slower than with the native Ca²⁺ as an oxygen evolving catalyst. Here, we use Density Functional Theory (DFT) to compare the energetics of the S₂ to S₃ transition in the Mn₄O₅Ca²⁺ and Mn₄O₅Sr²⁺ clusters. The calculations show that deprotonation of the water bound to Ca²⁺ (W3), required for the S₂ to S₃ transition, is energetically more favorable in Mn₄O₅Ca²⁺ than Mn₄O₅Sr²⁺. In addition, we have calculated the pK_a of the water that bridges Mn4 and the Ca²⁺/Sr²⁺ in the S₂ using continuum electrostatics. The calculations show that the pK_a is higher by 4 pH units in the Mn₄O₅Sr²⁺.

The oxygen evolving complex (OEC) is a unique natural bioinorganic cluster that catalyzes the water oxidation reaction in the 5-steps (S₀, S₁, S₂, S₃, S₄) Kok cycle.^{1,2} The core of the OEC contains a metal cluster of four Mn and one Ca²⁺ connected through bridging oxygens.²⁻⁴ Ca²⁺ depletion^{5,6} blocks the S₂-S₃ transition, while replacing Ca²⁺ with Sr²⁺ reduces the catalytic activity.⁷⁻¹⁰

Calcium and strontium belong to group 2 alkaline earth metals in the periodic table. Thus, they are chemically similar and have a stable oxidation state of +2. However, Ca²⁺ is a stronger Lewis acid, which indicates that aqua-Ca²⁺ compounds have a lower pK_a than aqua-Sr²⁺ (measured pK_a is 2 pH unit lower). This difference in proton affinity of the bound waters may be the reason for the difference in the catalytic activity in the Sr-substituted PSII.¹⁰⁻¹² Here, we use Density Functional Theory (DFT)

to compare the energetics of the S₂-S₃ transition in the native and Sr-substituted PSII.

Experimental¹³ and theoretical studies¹⁴⁻¹⁶ have proposed that the S₂-S₃ transition passes through an intermediate step in which the S₂ EPR signal changes from the multiline g=2 signal to the g=4.1. In the g=4.1 EPR state Mn1, Mn2, Mn3 are in the IV oxidation state, while Mn4 is in the III state (Fig 1).¹⁷ In the g=2 redox isomer M1 is Mn³⁺ while M4 is Mn⁴⁺. In addition, time-resolved photothermal beam deflection measurements suggest that a proton is released from the OEC or surroundings when the nearby Tyr, Y_z, is oxidized before Mn oxidation in the S₂-S₃ transition.^{18,19}

Based on classical electrostatic calculations and DFT study¹⁴, we previously proposed that the S₂-S₃ transition starts by the transition from g=2 to g=4.1 structure followed by deprotonation of the W3 Ca²⁺ ligand.²⁰ This is coupled to the protonation of HIS190 upon the oxidation of the secondary donor Y_z^{*}. The deprotonated W3 moves toward Mn4 adding the sixth ligand to its coordination shell to facilitate its oxidation to IV state. Similar mechanisms have been proposed by previous theoretical²¹⁻²⁴ and experimental¹⁰ studies.

Here, we compare the energies of two structures of the S₂ g=4.1 state, **A** in which HIS190 and W3 are neutral (Figure 1A) and **B** with protonated HIS190⁺ and W3 is a OH⁻ bridge between Mn4 and Ca²⁺ (Figure 1B) in both Mn₄O₅Ca²⁺ and Mn₄O₅Sr²⁺ clusters. The structures were optimized at the DFT level using the B3LYP

functional and 6-31G(d) basis sets for N, O, C and H atoms, while SDD are used for Mn, Ca and Sr. All the Mn ions are in the high spin state. Furthermore, the energies are compared using different levels of theory; B3LYP/6-31G+(d) and B97D/6-31G+(d).^{25,26}

The energy differences between the **A** and **B** states ($\Delta G_{(B-A)}$) at different level of theory are shown in (Table 1). In general, the **B** state (protonated HIS190 and hydroxyl on W3) is always more favorable for the $\text{Mn}_4\text{O}_5\text{Ca}^{2+}$ than the $\text{Mn}_4\text{O}_5\text{Sr}^{2+}$ cluster. The large energy difference obtained for the $\text{Mn}_4\text{O}_5\text{Sr}^{2+}$ cluster using B3LYP/6-31G(d) level of theory indicates the importance of including diffuse functions in the basis sets when modeling large ions. These diffuse functions provide flexible representation to the tail part of the atomic orbitals further from the nucleus.^{25,26}

Sr^{2+} is larger than Ca^{2+} by 0.1\AA , which elongates the interatomic distances between the Sr^{2+} and the rest of atoms in the Mn cluster. This is seen in the optimized structures of the **A** and **B** states with Ca^{2+} and Sr^{2+} clusters (Table 2). In addition, the dispersion interaction between the metal and the water ligand is expected to push the water away in case of Sr^{2+} , which will result in smaller electrostatic interactions and a higher pK_a . This is found for aqua- Ca^{2+} and aqua- Sr^{2+} compounds, where the water bound to Sr^{2+} have a higher pK_a than those bound to Ca^{2+} . Thus, the Sr^{2+} structure is more stable with neutral W3 (Figure 1A). However, with Ca^{2+} , W3 deprotonates forming a hydroxide that moves to bridge Mn4 and Ca^{2+} (Figure 1B).

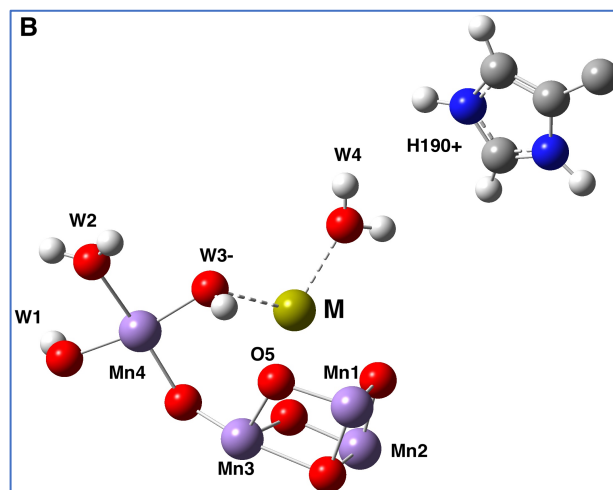
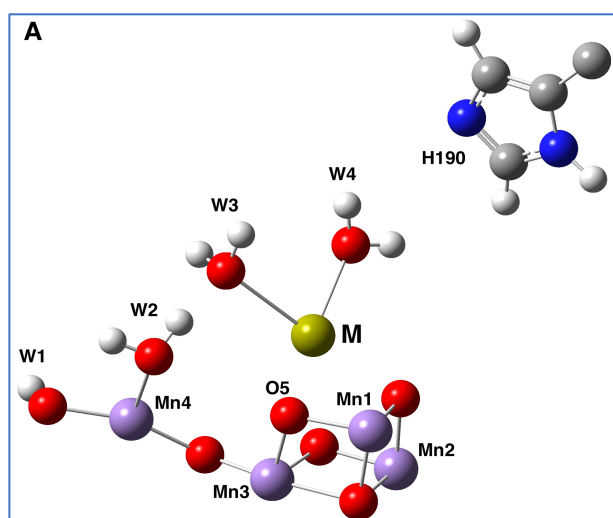


Figure 1. **A** represents the S_2 state with HIS190 neutral. **B** represents the S_2 state with HIS190^+ protonated. **M** is Ca^{2+} or Sr^{2+} . Mn1, Mn2, Mn3 are in the IV oxidation state. Mn4 is III. The rest of atoms in the model were removed for clarity.

The optimized DFT structures show that Mn-Sr²⁺ distances are in general longer than Mn-Ca²⁺. In the **A** state the Sr²⁺-W3(HOH) distance is longer by 0.1\AA than Ca²⁺-W3(HOH), while in the **B** state the Sr²⁺-W3(OH)⁻ distance is 0.2\AA longer. The Mn1 to Ca²⁺, is longer because Ca²⁺ moves significantly toward Mn4 after the deprotonation of W3.

Table 1. The $\Delta G_{(B-A)}$ DFT energies.

	B3LYP/ 6-31G(d)	B3LYP/6- 31G+(d)	B97D/6- 31G+(d)
$\text{Mn}_4\text{O}_5\text{Ca}^{2+}$	-2.3	-8.7	-6.8
$\text{Mn}_4\text{O}_5\text{Sr}^{2+}$	13.0	-8.0	-6.4

Energy differences are expressed in Kcal/mol. The transition from **A** to **B** state is more favorable in the $\text{Mn}_4\text{O}_5\text{Ca}^{2+}$ cluster than the $\text{Mn}_4\text{O}_5\text{Sr}^{2+}$

To further compare the $\text{Mn}_4\text{O}_5\text{Ca}^{2+}$ the $\text{Mn}_4\text{O}_5\text{Sr}^{2+}$, we calculated the pK_a of W3 in the **A** state for both clusters using continuum electrostatics.^{27,28} W3 has a pK_a of 6.5 for the $\text{Mn}_4\text{O}_5\text{Ca}^{2+}$ and 10.3 in the $\text{Mn}_4\text{O}_5\text{Sr}^{2+}$. The lower pK of W3 in Ca^{2+} structure is expected as W3 is significantly closer to the positively charged ions (Ca^{2+} , Mn4(III) and Mn1(IV)) (Table 2). This conclusion is supported by the DFT calculations, which show that **B** is lower energy than **A** indicating the easier deprotonation in case of the $\text{Mn}_4\text{O}_5\text{Ca}^{2+}$.

An open question is what the source of the proton which is released after Y_z is oxidized but before the OEC

advances to the S₃ state.^{3,29} As there are no protons bound to the bridging oxygens in the S₂ state, the donors are likely to be terminal water ligands bound to Mn4 water^{30,31} or to Ca.³² Previous studies have shown the Mn4-bound water W1 to be upon the formation of tyrosyl radical, however the proton is trapped by the nearby acceptor D61.^{16,33,34}

The present study utilizes the S₂ g=4.1 models for Ca²⁺ and Sr²⁺ to understand the nature of deprotonation event. Our DFT calculations support the deprotonation of W3 in the S₂ to S₃ transition, which is also supported by the XFEL structures comparing S₁, S₂ and S₃ states.²⁸

Table 2. Interatomic distances in A and B states.

	A		B	
	Ca ²⁺	Sr ²⁺	Ca ²⁺	Sr ²⁺
Mn1	2.50	3.58	3.49	3.67
Mn4	4.35	4.51	3.58	2.64
W3	2.55	2.66	2.39	2.58
W4	2.33	2.50	2.35	2.53
O5	2.66	2.78	2.66	2.77

All distances are reported in Å. In general, the interatomic distances are longer for Sr²⁺.

Supporting Information

The Supporting Information includes details of the continuum electrostatic calculations and the optimized atomic coordinates of the optimized A and B structures.

Acknowledgements

The authors acknowledge computational resources from the support by the U.S. Department of Energy, Office of Science, Office of Basic Energy Sciences, Division of Chemical Sciences, Geosciences, and Biosciences via Grants DESC0001423 (M.R.G. and V.S.B.), DE-FG02-05ER15646 (G.W.B.).

References:

- (1) Vinyard, D. J.; Brudvig, G. W. Progress toward a Molecular Mechanism of Water Oxidation in Photosystem II. *Annu. Rev. Phys. Chem.* **2017**, *68* (1), 101–116. <https://doi.org/10.1146/annurev-physchem-052516-044820>.
- (2) Kern, J.; Chatterjee, R.; Young, I. D.; Fuller, F. D.; Lassalle, L.; Ibrahim, M.; Gul, S.; Fransson, T.; Brewster, A. S.; Alonso-Mori, R.; Hussein, R.; Zhang, M.; Douthit, L.; de Lichtenberg, C.; Cheah, M. H.; Shevela, D.; Wersig, J.; Seuffert, I.; Sokaras, D.; Pastor, E.; Weninger, C.; Kroll, T.; Sierra, R. G.; Aller, P.; Butryn, A.; Orville, A. M.; Liang, M.; Batyuk, A.; Koglin, J. E.; Carbajo, S.; Boutet, S.; Moriarty, N. W.; Holton, J. M.; Dobbek, H.; Adams, P. D.; Bergmann, U.; Sauter, N. K.; Zouni, A.; Messinger, J.; Yano, J.; Yachandra, V. K. Structures of the Intermediates of Kok's Photosynthetic Water Oxidation Clock. *Nature* **2018**, *563* (7731), 421–425. <https://doi.org/10.1038/s41586-018-0681-2>.
- (3) Suga, M.; Akita, F.; Yamashita, K.; Nakajima, Y.; Ueno, G.; Li, H.; Yamane, T.; Hirata, K.; Umena, Y.; Yonekura, S.; Yu, L.-J.; Murakami, H.; Nomura, T.; Kimura, T.; Kubo, M.; Baba, S.; Kumasaka, T.; Tono, K.; Yabashi, M.; Isobe, H.; Yamaguchi, K.; Yamamoto, M.; Ago, H.; Shen, J.-R. An Oxyl/Oxo Mechanism for Oxygen-Oxygen Coupling in PSII Revealed by an x-Ray Free-Electron Laser. *Science* **2019**, *366* (6463), 334–338. <https://doi.org/10.1126/science.aax6998>.
- (4) Umena, Y.; Kawakami, K.; Shen, J.-R.; Kamiya, N. Crystal Structure of Oxygen-Evolving Photosystem II at a Resolution of 1.9 Å. *Nature* **2011**, *473* (7345), 55–60. <https://doi.org/10.1038/nature09913>.
- (5) Boussac, A.; Zimmermann, J. L.; Rutherford, A. W. EPR Signals from Modified Charge Accumulation States of the Oxygen Evolving Enzyme in Ca²⁺-Deficient Photosystem II. *Biochemistry* **1989**, *28* (23), 8984–8989. <https://doi.org/10.1021/bi00449a005>.
- (6) Latimer, M. J.; DeRose, V. J.; Yachandra, V. K.; Sauer, K.; Klein, M. P. Structural Effects of Calcium Depletion on the Manganese Cluster of Photosystem II: Determination by X-Ray Absorption Spectroscopy. *J Phys Chem B* **1998**, *102*, 8257–8265.
- (7) Ghanotakis, D. F.; Babcock, G. T.; Yocum, C. F. Calcium Reconstitutes High Rates of Oxygen Evolution in Polypeptide Depleted Photosystem II Preparations. *FEBS Letters* **1984**, *167* (1), 127–130. [https://doi.org/10.1016/0014-5793\(84\)80846-7](https://doi.org/10.1016/0014-5793(84)80846-7).
- (8) Boussac, A.; Rutherford, A. W. Nature of the Inhibition of the Oxygen-Evolving Enzyme of Photosystem II Induced by Sodium Chloride Washing and Reversed by the Addition of Calcium²⁺ or Strontium²⁺. *Biochemistry* **1988**, *27* (9), 3476–3483. <https://doi.org/10.1021/bi00409a052>.
- (9) Boussac, A.; Rappaport, F.; Carrier, P.; Verbatz, J.-M.; Gobin, R.; Kirilovsky, D.; Rutherford, A. W.; Sugiura, M. Biosynthetic Ca²⁺/Sr²⁺ Exchange in the Photosystem II Oxygen-Evolving Enzyme of *Thermosynechococcus Elongatus*. *J. Biol.*

- Chem.* **2004**, 279 (22), 22809–22819.
<https://doi.org/10.1074/jbc.M401677200>.
- (10) Kim, C. J.; Debus, R. J. Evidence from FTIR Difference Spectroscopy That a Substrate H₂O Molecule for O₂ Formation in Photosystem II Is Provided by the Ca Ion of the Catalytic Mn₄CaO₅ Cluster. *Biochemistry* **2017**, 56 (20), 2558–2570. <https://doi.org/10.1021/acs.biochem.6b01278>.
- (11) Koua, F. H. M.; Umena, Y.; Kawakami, K.; Shen, J.-R. Structure of Sr-Substituted Photosystem II at 2.1 Å Resolution and Its Implications in the Mechanism of Water Oxidation. *Proc. Natl. Acad. Sci. U.S.A.* **2013**, 110 (10), 3889–3894. <https://doi.org/10.1073/pnas.1219922110>.
- (12) Vogt, L.; Ertem, M. Z.; Pal, R.; Brudvig, G. W.; Batista, V. S. Computational Insights on Crystal Structures of the Oxygen-Evolving Complex of Photosystem II with Either Ca²⁺ or Sr²⁺ Substituted by Sr²⁺. *Biochemistry* **2015**, 54 (3), 820–825. <https://doi.org/10.1021/bi5011706>.
- (13) Boussac, A.; Ugur, I.; Marion, A.; Sugiura, M.; Kaila, V. R. I.; Rutherford, A. W. The Low Spin - High Spin Equilibrium in the S₂-State of the Water Oxidizing Enzyme. *Biochim Biophys Acta Bioenerg* **2018**, 1859 (5), 342–356. <https://doi.org/10.1016/j.bbabi.2018.02.010>.
- (14) Amin, M.; Kaur, D.; Yang, K. R.; Wang, J.; Mohamed, Z.; Brudvig, G. W.; Gunner, M. R.; Batista, V. Thermodynamics of the S₂ to S₃ State Transition of the Oxygen-Evolving Complex of Photosystem II. *Phys Chem Chem Phys* **2019**, 21 (37), 20840–20848. <https://doi.org/10.1039/c9cp02308a>.
- (15) Kaur, D.; Szejgis, W.; Mao, J.; Amin, M.; Reiss, K. M.; Askerka, M.; Cai, X.; Khaniya, U.; Zhang, Y.; Brudvig, G. W.; Batista, V. S.; Gunner, M. R. Relative Stability of the S₂ Isomers of the Oxygen Evolving Complex of Photosystem II. *Photosyn. Res.* **2019**, 141 (3), 331–341. <https://doi.org/10.1007/s11120-019-00637-6>.
- (16) Narzi, D.; Bovi, D.; Guidoni, L. Pathway for Mn-Cluster Oxidation by Tyrosine-Z in the S₂ State of Photosystem II. *Proc. Natl. Acad. Sci. U.S.A.* **2014**, 111 (24), 8723–8728. <https://doi.org/10.1073/pnas.1401719111>.
- (17) Zimmermann, J. L.; Rutherford, A. W. Electron Paramagnetic Resonance Properties of the S₂ State of the Oxygen-Evolving Complex of Photosystem II. *Biochemistry* **1986**, 25 (16), 4609–4615. <https://doi.org/10.1021/bi00364a023>.
- (18) Zaharieva, I.; Dau, H. Energetics and Kinetics of S-State Transitions Monitored by Delayed Chlorophyll Fluorescence. *Front Plant Sci* **2019**, 10, 386. <https://doi.org/10.3389/fpls.2019.00386>.
- (19) Zaharieva, I.; Dau, H.; Haumann, M. Sequential and Coupled Proton and Electron Transfer Events in the S₂ → S₃ Transition of Photosynthetic Water Oxidation Revealed by Time-Resolved X-Ray Absorption Spectroscopy. *Biochemistry* **2016**, 55 (50), 6996–7004. <https://doi.org/10.1021/acs.biochem.6b01078>.
- (20) Pérez-Navarro, M.; Neese, F.; Lubitz, W.; Pantazis, D. A.; Cox, N. Recent Developments in Biological Water Oxidation. *Curr Opin Chem Biol* **2016**, 31, 113–119. <https://doi.org/10.1016/j.cbpa.2016.02.007>.
- (21) Bovi, D.; Narzi, D.; Guidoni, L. The S₂ State of the Oxygen-Evolving Complex of Photosystem II Explored by QM/MM Dynamics: Spin Surfaces and Metastable States Suggest a Reaction Path towards the S₃ State. *Angew. Chem.* **2013**, 52 (45), 11744–11749. <https://doi.org/10.1002/anie.201306667>.
- (22) Shoji, M.; Isobe, H.; Yamaguchi, K. QM/MM Study of the S₂ to S₃ Transition Reaction in the Oxygen-Evolving Complex of Photosystem II. *Chem. Phys. Lett.* **2015**, 636, 172–179. <https://doi.org/10.1016/j.cplett.2015.07.039>.
- (23) Isobe, H.; Shoji, M.; Shen, J.-R.; Yamaguchi, K. Strong Coupling between the Hydrogen Bonding Environment and Redox Chemistry during the S₂ to S₃ Transition in the Oxygen-Evolving Complex of Photosystem II. *J Phys Chem B* **2015**, 119 (43), 13922–13933. <https://doi.org/10.1021/acs.jpcc.5b05740>.
- (24) Ugur, I.; Rutherford, A. W.; Kaila, V. R. I. Redox-Coupled Substrate Water Reorganization in the Active Site of Photosystem II—The Role of Calcium in Substrate Water Delivery. *Biochim Biophys Acta Bioenerg* **2016**, 1857 (6), 740–748. <https://doi.org/10.1016/j.bbabi.2016.01.015>.
- (25) Grimme, S. Semiempirical GGA-Type Density Functional Constructed with a Long-Range Dispersion Correction. *J Comput Chem* **2006**, 27 (15), 1787–1799. <https://doi.org/10.1002/jcc.20495>.
- (26) Becke, A. D. Density-functional Thermochemistry. III. The Role of Exact Exchange. *J. Chem. Phys.* **1993**, 98 (7), 5648–5652. <https://doi.org/10.1063/1.464913>.
- (27) Amin, M.; Vogt, L.; Szejgis, W.; Vassiliev, S.; Brudvig, G. W.; Bruce, D.; Gunner, M. R. Proton-Coupled Electron Transfer during the S-State Transitions of the Oxygen-Evolving Complex of Photosystem II. *J. Phys. Chem. B* **2015**, 119 (24), 7366–7377. <https://doi.org/10.1021/jp510948e>.
- (28) Song, Y.; Mao, J.; Gunner, M. R. MCCE2: Improving Protein PK_a Calculations with Extensive Side Chain Rotamer Sampling. *J. Comput. Chem.* **2009**, 30 (14), 2231–2247. <https://doi.org/10.1002/jcc.21222>.
- (29) Askerka, M.; Wang, J.; Vinyard, D. J.; Brudvig, G. W.; Batista, V. S. S₃ State of the O₂-Evolving

- Complex of Photosystem II: Insights from QM/MM, EXAFS, and Femtosecond X-Ray Diffraction. *Biochemistry* **2016**, *55* (7), 981–984. <https://doi.org/10.1021/acs.biochem.6b00041>.
- (30) Askerka, M.; Vinyard, D. J.; Brudvig, G. W.; Batista, V. S. NH₃ Binding to the S₂ State of the O₂-Evolving Complex of Photosystem II: Analogue to H₂O Binding during the S₂ → S₃ Transition. *Biochemistry* **2015**, *54* (38), 5783–5786. <https://doi.org/10.1021/acs.biochem.5b00974>.
- (31) Wang, J.; Askerka, M.; Brudvig, G. W.; Batista, V. S. Crystallographic Data Support the Carousel Mechanism of Water Supply to the Oxygen-Evolving Complex of Photosystem II. *ACS Energy Lett* **2017**, *2* (10), 2299–2306. <https://doi.org/10.1021/acsenergylett.7b00750>.
- (32) Kim, C. J.; Debus, R. J. One of the Substrate Waters for O₂ Formation in Photosystem II Is Provided by the Water-Splitting Mn₄CaO₅ Cluster's Ca²⁺ Ion. *Biochemistry* **2019**, *58* (29), 3185–3192. <https://doi.org/10.1021/acs.biochem.9b00418>.
- (33) Retegan, M.; Krewald, V.; Mamedov, F.; Neese, F.; Lubitz, W.; Cox, N.; Pantazis, D. A. A Five-Coordinate Mn(IV) Intermediate in Biological Water Oxidation: Spectroscopic Signature and a Pivot Mechanism for Water Binding. *Chem. Sci.* **2015**, *7* (1), 72–84. <https://doi.org/10.1039/C5SC03124A>.
- (34) Kawashima, K.; Takaoka, T.; Kimura, H.; Saito, K.; Ishikita, H. O₂ Evolution and Recovery of the Water-Oxidizing Enzyme. *Nat Commun* **2018**, *9* (1), 1247. <https://doi.org/10.1038/s41467-018-03545-w>.